Indones. J. Chem., 2023, 23 (6), 1567 - 1583

1567

Organic Geochemical Characteristics of Ngrayong Formation Polaman Sediment Rock, Northeast Java Basin-Indonesia

Yulfi Zetra[1*], Rafwan Year Perry Burhan[1], Sulistiyono Sulistiyono[2], Arizal Firmansyah[3], and Darin Salsabila[1]

[1]Department of Chemistry, Faculty of Science and Data Analytics, Institut Teknologi Sepuluh Nopember Surabaya, Kampus ITS Keputih, Surabaya 60111, Indonesia

[2]Polytechnic of Energy and Mineral Akamigas, Jl. Gajah Mada No. 38, Cepu 58315, Indonesia

[3]Department of Chemistry Education, Faculty of Science and Technology, Universitas Islam Negeri Walisongo Semarang, Kampus 3, Ngaliyan, Semarang 50185, Indonesia

Abstract: *A study of the sedimentary rocks of the Ngrayong formation has been carried out on five samples from the Polaman outcrop point to determine the potential of coal as a source rock for producing oil and gas through GC-MS analysis. Biomarker analysis shows the presence of n-alkanes (C_{16}-C_{36}) with a bimodal distribution, indicating that the source of organic material in sedimentary rocks comes from bacteria, algae, and vascular plants, which is supported by several parameters such as CPI, OEP, LHCPI, wax index, ACL and AlkTerr values. This dominant source of terrigenous organic matter is also proven by the TAR value, C_{31}/C_{19}, C_{29}/C_{17} ratio, and several aromatic compounds and their derivatives. Bacterial input as an organic source of allouchtonic sedimentary rocks is also proven by the presence of hopanoid, de-A-lupane biomarkers, and C_{17}/C_{31} ratio. The oxic deposition environment is indicated by the Pr/Ph ratio. CPI and OEP parameters, C_{29} bb/ab ratio > 0.15 and C_{31} 22S/(22S+22R) < 1 indicate low maturity of the sediment sample. Several parameters and the presence of biomarkers stated above conclude that Ngrayong coal as a source rock has the potential to produce oil and gas.*

Keywords: *aliphatic hydrocarbons; aromatic hydrocarbons; biomarkers; Ngrayong formation; Polaman sediments*

■ INTRODUCTION

Oil and gas exploration is inseparable from the petroleum system. This concept is an integration of the source rock, reservoir, migration, trapping model, and the presence of overburden. The research area is centered on the northern part of the East Java Basin. Several types of source rock commonly exist in this basin, including lacustrine (Ngimbang formation), shale (Kujung formation), and coal (Ngrayong formation), which is considered as the secondary source of hydrocarbons. The Middle Miocene-aged Ngrayong formation that was deposited in a tidal area has transgressed into the middle to outer exposure environment. The dominance of lithology was in the form of clean sand, generating a main

reservoir in the Rembang zone, especially the Cepu district. The Ngrayong formation can be represented as an outcrop on the Braholo river and the Polaman outcrop in the previous quartz sandstone mine. The Polaman outcrop occurred in the Middle Miocene, with the clay stone composed at the bottom. This outcrop enables it to turn upwards, becoming an interlude between sandstone and shale. The PLM 1, PLM 2, PLM 3, PLM 4, and PLM 5 samples were taken at five different points from the Polaman outcrop. The shale rock exhibited a dark color and contained organic material. These two lithologies are promising candidates for source rock based on petroleum systems [1-2]. Several researchers have reported organic geochemical characteristics through biomarker analysis to determine

the source of organic compounds, thermal maturity, and depositional environment of a geological sediment sample [3]. The dominance of long-chain *n*-alkanes homologues over short-chain *n*-alkanes confirmed vascular plants as the source of organic compounds. The presence of hopanoid compounds such as 17α(*H*),21β(*H*)-hopane, 17β(*H*),21α(*H*)-hopane, and 17α(*H*),21β(*H*)-30-homohopane with 22*S* and 22*R* configurations assigned the contribution of bacteria during the process of organic compounds formation. Hopanoid compounds were also an indicator of the thermal maturity of a sediment. The dominance of 17α(*H*),21β(*H*)-homohopane (22*R*) against 17α(*H*),21β(*H*)-homohopane (22*S*) was a sign of low maturity [4-8]. Environmental conditions of sediment deposition can be investigated through the distribution of pristane and phytane compounds [6,9].

The biomarker analysis provided information on the organic geochemical allowing the hydrocarbon potential hydrocarbons in the Polaman sediments of the Ngrayong formation, Northeast Java Basin. This analysis was adopted due to its feasibility and accuracy since the biomarker inferred the characteristics of oil and gas in the reservoir. In addition, this analysis was mostly applied in the oil and gas exploration field. Biomarkers were extracted using the Soxhlet method and fractioned over TLC SiO$_2$ GF$_{254}$. Extraction and fractionation results were further identified by gas chromatography-mass spectrometry (GC-MS).

■ EXPERIMENTAL SECTION

Materials

Sediment samples were obtained from five different coordinate points with characteristics as mentioned in Table 1. The five sedimentary rock objects are outcrop pattern sediment samples. The organic solvents used in this study were *n*-hexane and dichloromethane (grade pro analysis, Sigma-Aldrich). Other materials were copper powder and silica gel GF$_{254}$ TLC plate (Sigma-Aldrich).

Instrumentation

Identification of biomakers in this work used the Agilent D5975C GC-MS with column type of HP-5MS (60 μm × 250 μm × 0.33 μm).

Table 1. Characteristics of PLM sediment samples PLM 1-PLM 5

Sample number	Coordinate		Rock description
	Latitude	Longitude	
PLM 1	6°54'11.02"S	111°26'30.17"E	Type: Shale stone Color: Brownish gray Grain size: Very fine sand Evolved sedimentary structure: Flake General composition: Silica cement Presence of mature organic/fossil: Few fossils form
PLM 2	6°54'11.11"S	111°26'30.14"E	Type: Shale stone Color: Light gray Grain size: Very fine sand Developed sedimentary structure: Slightly laminated General composition: Silica cement Organic/fossil maturity state: Organic maturity present
PLM 3	6°54'11.20"S	111°26'30.13"E	Type: Clay Color: Light gray Granule Size: Clay Evolved sedimentary structure: Conchoidal General composition: Silica cement Organic/fossil maturity state: Slightly organic maturity

Sample number	Coordinate		Rock description
	Latitude	Longitude	
PLM 4	6°54'11.28"S	111°26'30.11"E	Type: Shale Color: Gray Grain size: Very fine sand Evolved sedimentary structure: Laminate General composition: Silica cement Organic/fossil maturity state: Carbon strike
PLM 5	6°54'11.36"S	111°26'30.09"E	Type: Shale Color: Blackish gray Grain size: Very fine sand Evolved sedimentary structure: Flake General composition: Silica cement Organic/fossil maturity state: Carbon strike

Procedure

About 100 mg of Polaman sediment was extracted in dichloromethane to obtain a total organic extract. The organic extract was fractionated by the thin layer chromatography (TLC) method with *n*-hexane as eluent to separate aliphatic, aromatic, and polar hydrocarbon fractions. The aromatic hydrocarbon fraction was then desulfurized using copper (Cu) powder. The aliphatic and aromatic fractions were further analyzed using GC-MS. Each Polaman sediment sample was dissolved in *n*-hexane and injected into GC-MS afterward [8].

Helium as carrier gas, flowed at the rate of 1 mL/min. The oven temperature was programmed with an initial temperature at 70 °C held for 3 min, ramped at 10 °C/min to 160 °C, and a final ramp of 3 °C/min to 320 °C maintained for 27.5 min. The sample was injected with a split ratio of 50:1, and analysis was conducted with a solvent delay of 4 min. The mass spectrometer is operated with an electron energy of 70 eV. The data obtained were further analyzed with Enhanced Chemstation software. The compounds were identified based on the specific *m/z* fragmentogram, retention time pattern, and mass spectrum fragmentation. The identification results were compared to previous studies [4,10-13].

■ RESULTS AND DISCUSSION
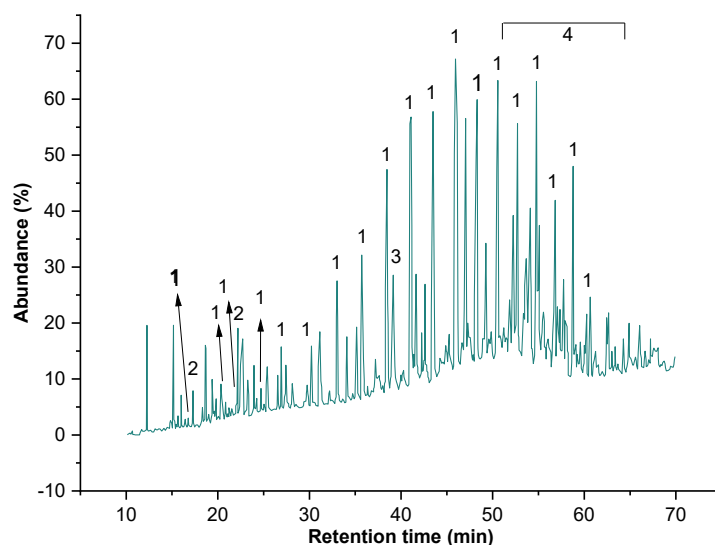
Aliphatic Hydrocarbon Fraction

The result of biomarker aliphatic hydrocarbon fraction identification of sediment samples using GC-MS is depicted in Fig. 1. It was observed that all samples contained *n*-alkanes, isoprenoids, and triterpenoids. The *n*-alkanes were found in PLM 1-5, while isoprenoids only existed in samples PLM 2 and PLM 3.
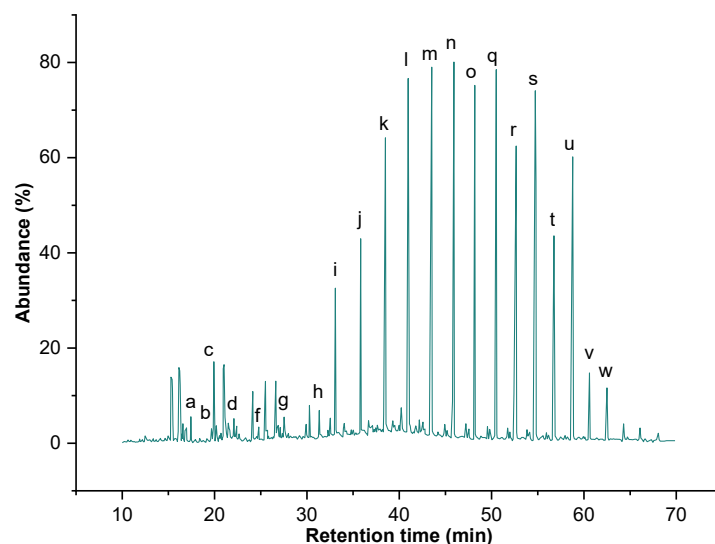
n-*Alkanes and isoprenoids*

The *n*-alkanes and op were identified based on the specific fragmentogram *m/z* 57 that showed the presence of short-chain (n-C_{16}–n-C_{20}), medium (n-C_{21}–n-C_{25}), and long-chain (n-C_{26}–n-C_{37}) of alkanes over bimodal distribution (Fig. 2). The length of the alkane chain assigned the organic matter source, where the short chain represented bacteria (i.e. cyanobacteria) and algae. The medium chain confirmed the contribution of bacteria, algae, and machropyte, including the submerged and floating ones. In addition, the vascular plant as the source of organic matter was affirmed by the long-chain alkane [14-20].

All samples exhibited a wide range of alkanes, with the highest and the lowest abundance being n-C_{27} and n-C_{16}, respectively. This result concludes that the organic matter source originated from bacteria, algae, and vascular plants, as found in sediments in Teluk Bunai, eastern Malaysia [20]. In terms of isoprenoid, pristane was observed in PLM 2, and phytane was found in PLM 2 as well as PLM 3. The abundance of alkane and isoprenoid is illustrated in Table 2. This table explains several parameters, i.e., carbon preference index (CPI), odd/even predominance (OEP), low-to-high chain carbon preference index (LHCPI), Pr/Ph, Pr/n-C_{17}, Ph/n-C_{18},

Fig 1. Total ion chromatogram of aliphatic hydrocarbon fraction of PLM sediment samples 1-5. (1) *n*-alkane, (2) isoprenoids, (3) sesterterpenoids, and (4) pentacyclic triterpenoids

Fig 2. Fragmentogram of *n*-alkane and isoprenoid compounds on *m/z* 57 sediment samples PLM 1-5

Table 2. The abundance of aliphatic hydrocarbon fractions in PLM sediment samples 1-5

Peak	Compound	Molecular formula	Base peak (*m/z*)	M+ (*m/z*)	Composition (%) PLM-1	PLM-2	PLM-3	PLM-4	PLM-5
n-alkanes, and isoprenoids									
a	*n*-C_{16}	$C_{16}H_{34}$	57	226	0.21	0.10	-	-	-
b	*n*-C_{17}	$C_{17}H_{36}$	57	240	0.30	0.29	0.41	-	-
c	pristane	$C_{19}H_{40}$	57	268	-	0.21	0.58	-	-
d	*n*-C_{18}	$C_{18}H_{38}$	57	254	0.42	0.46	0.54	-	-
e	phytane	$C_{20}H_{42}$	57	282	-	0.17	-	-	-
f	*n*-C_{19}	$C_{19}H_{40}$	57	268	0.27	0.51	0.46	0.14	0.20
g	*n*-C_{20}	$C_{20}H_{42}$	57	282	0.59	1.20	0.87	0.30	0.34

Peak	Compound	Molecular formula	Base peak (*m/z*)	M⁺ (m/z)	Composition (%)				
					PLM-1	PLM-2	PLM-3	PLM-4	PLM-5
h	n-C$_{21}$	C$_{21}$H$_{44}$	57	296	0.62	1.44	0.93	0.59	0.66
i	n-C$_{22}$	C$_{22}$H$_{46}$	57	310	3.34	3.54	3.73	2.42	2.56
j	n-C$_{23}$	C$_{23}$H$_{48}$	57	324	4.77	4.72	4.17	3.59	3.39
k	n-C$_{24}$	C$_{24}$H$_{50}$	57	338	7.93	7.79	7.54	6.57	6.58
l	n-C$_{25}$	C$_{25}$H$_{52}$	57	352	9.31	10.65	9.72	10.30	9.00
m	n-C$_{26}$	C$_{26}$H$_{54}$	57	366	9.91	10.90	10.53	9.43	10.86
n	n-C$_{27}$	C$_{27}$H$_{56}$	57	380	10.14	12.31	10.86	11.44	11.71
o	n-C$_{28}$	C$_{28}$H$_{58}$	57	394	8.95	9.98	9.37	9.57	10.35
p	n-C$_{29}$	C$_{29}$H$_{60}$	57	408	9.80	9.18	9.42	10.15	10.93
q	n-C$_{30}$	C$_{30}$H$_{62}$	57	422	7.52	7.36	6.92	8.17	8.27
r	n-C$_{31}$	C$_{31}$H$_{64}$	57	436	9.94	7.87	9.87	10.68	10.41
s	n-C$_{32}$	C$_{32}$H$_{66}$	57	450	5.04	4.26	4.82	5.52	4.92
t	n-C$_{33}$	C$_{33}$H$_{68}$	57	464	7.41	5.25	4.84	7.16	6.17
u	n-C$_{34}$	C$_{34}$H$_{70}$	57	478	1.72	1.83	2.14	2.06	1.75
v	n-C$_{35}$	C$_{35}$H$_{72}$	57	492	1.35	-	1.65	1.31	1.28
w	n-C$_{36}$	C$_{36}$H$_{74}$	57	506	0.47	-	0.63	0.19	0.61
x	n-C$_{37}$	C$_{37}$H$_{76}$	57	520	-	-	-	0.40	-
Sesterterpenoids									
a	de-A-lupane	C$_{24}$H$_{42}$	123	330	37.82	17.68	24.21	13.16	28.09
Pentacyclic Triterpenoids									
b	17α(*H*)-22,29,30-trisnorhopane (Tm)	C$_{27}$H$_{46}$	191	370	2.36	-	-	-	3.25
c	17β(*H*)-22,29,30-trisnorhopane	C$_{27}$H$_{46}$	191	370	15.40	8.64	8.80	18.59	14.83
d	olean-12-ene	C$_{30}$H$_{50}$	218	410	5.44	43.27	23.70	-	3.18
e	17α(*H*),21β(*H*)-30-norhopane	C$_{29}$H$_{50}$	191	398	-	-	-	10.19	-
f	17β(*H*),21β(*H*)-30-norhopane	C$_{29}$H$_{50}$	177	398	8.07	9.18	6.11	22.78	8.78
g	17β(*H*), 21β(*H*)-hopane	C$_{30}$H$_{52}$	191	412	3.78	-	2.89	8.85	5.44
h	17β(*H*),21α(*H*)-30-normorethane	C$_{29}$H$_{50}$	177	398	11.33	-	10.98	10.38	12.49
i	17α(*H*),21β(*H*)-30-homohopane (22*S*)	C$_{31}$H$_{54}$	191	426	2.77	4.09	5.29	5.68	4.42
j	17α(*H*),21β(*H*)-30-homohopane (22*R*)	C$_{31}$H$_{54}$	191	426	10.13	7.40	11.93	10.37	10.41
k	gamaserane	C$_{30}$H$_{52}$	191	412	-	6.90	-	-	-
l	17β(*H*),21β(*H*)-30-homohopane	C$_{31}$H$_{54}$	205	426	2.91	2.85	6.09	-	9.11

wax index, average chain length (ACL), Paq, terrigenous/aquatic ratio (TAR), low molecular weight to high molecular weight (LMW/HMW), alkane terrigenous (AlkTerr), n-C$_{29}$/n-C$_{17}$, and n-C$_{31}$/n-C$_{19}$ [19,21].

The maturity, organic matter source, and sediment were represented by the parameters mentioned in Table 3. CPI assigned the organic compound source. When the CPI value was lower than one indicated bacteria and algae, while the higher value affirmed the vascular plants. All samples possessed CPI values higher than 1, confirming the vascular plant as the major source. The highest CPI value of 1.35 belonged to PLM 4, and the lowest value of 1.00 was exhibited by PLM 2. The same result was also found in the investigation of the Yellow River in China [17,22]. The CPI index also indicated the maturity of sediment samples; higher CPI pointed to a higher

1572

Indones. J. Chem., 2023, 23 (6), 1567 - 1583

maturity [23]. All samples possessed CPI values lower than 1, confirming the low maturity of coal [6,24-25].

The OEP value of sediments was found to be lower than 1 and dominated by odd carbon, which confirms aquatic creatures as the main source of organic compounds [11,23,26]. All samples showed a narrow range of OEP values from 1.14–1.20, confirming vascular plants as the major organic source origin, as observed in the Posidonia and Hils Syncline sediment samples in Germany, and eastern Junggar, China [9,11,23,26].

The LHCPI also confirmed the organic compound source through the presence of alkane in sediment. The vascular plant's role in the formation of organic sources was confirmed by LHCP value of below one. Beyond that, the short chain was claimed by the high LHCPI value that points to the role of bacteria. The LHCPI also provided information on the maturity of Polaman sediments. It was confirmed that the major organic compound source was vascular plants, as affirmed by all samples possessing LHCPI lower than one, mentioned on Teluk Brunei sediment, Malaysia [20]. Another parameter was the wax index as an affirmation of the organic source. The dominance of short-chain n-alkanes over long chains was inferred by a wax value of higher than 1, confirming the

bacteria and algae as the main contributors [8]. All samples have a wax index lower than one, with the highest wax index of 0.15 and the lowest of 0.26. This value informed that the source of organic compounds was dominated by vascular plants [8].

Average chain length enabled the prediction of organic sources through the abundance of odd-chain alkanes (C_{25}-C_{33}) [22,27]. The benchmark ACL value was 28; the value below this point represented the wax layer. Inversely, the ACL value above 28 pointed to the role of vascular plants. Specifically, n-C_{31} and n-C_{33} confirmed that grass and herbs are the origin of organic compounds. Generally, all samples provided generated ACL values in the span of 28.32 to 28.83, confirming the wax and vascular plant as the source of the organic compound. This result was also observed in the study of Guanabara sediment [22,28].

The Paq parameter value represents the origin of the coal. The Paq values of PLM 1, PLM 2, PLM 3, PLM 4, and PLM 5 are 0.42, 0.47, 0.42, 0.40, and 0.37, respectively (Fig. 2). Paq values < 0.1 were for vascular plants, 0.1–0.4 for emergent macrophytes, and 0.4–1.0 for submerged/floating macrophytes [11,16,18-19]. Coal samples from PLM 1-4 were indicated to originate from

Table 3. Parameter values of n-alkane, isoprenoid, and triterpenoid compounds in PLM sediments 1-5

Parameter	Sample				
	PLM-1	PLM-2	PLM-3	PLM-4	PLM-5
CPI	1.30	1.22	1.23	1.35	1.26
OEP	1.19	-	1.14	1.20	1.14
LHCPI	0.03	0.03	0.05	-	-
Pr/Ph	-	1.26	-	-	-
Pr/n-C_{17}	-	0.73	-	-	-
Ph/n-C_{18}	-	0.36	-	-	-
Wax index	0.21	0.26	0.25	0.15	0.15
ACL	28.83	28.32	28.52	28.72	28.71
Paq	0.42	0.47	0.42	0.40	0.37
TAR	-	36.92	-	-	-
LMW/HMW	-	0.02	-	-	-
AlkTerr	0.39	0.34	-	-	-
n-C_{29}/n-C_{17}	32.67	32.11	22.71	-	-
n-C_{31}/n-C_{19}	36.81	15.46	21.66	75.35	51.35
n-C_{17}/n-C_{31}	0.03	0.03	0.04	-	-
C_{29} $\beta\beta/\alpha\beta$				2.24	
C_{31} 22S/(22S + 22R)	0.22	0.33	0.31	0.35	0.30

submerged/floating macrophytes, similar to the sediments of the Cochin mangrove forest on the west coast of India, while PLM 5 came from emergent macrophytes [29].

The relationship of organic matter sources with aquatic and terrestrial environments was evaluated through the TAR parameter, which was obtained from the ratio of the total n-alkanes C_{27}, C_{29}, and C_{31} to the total n-alkanes C_{15}, C_{17}, and C_{19}. The TAR value of PLM 2 was 36.92, indicating a higher contribution of vascular plants in the terrestrial environment [11,19]. Parameter LMW/HMW was calculated by comparing the abundance of n-alkane $\leq C_{21}$ with n-alkane $\geq C_{21}$ as well as coastal sediments of St. Lawrence Estuary and Gulf, Quebec, Canada [30]. The PLM 2 sample has an LMW/HMW value of 0.02 (< 1) (Table 3), confirming that the organic matter comes from vascular plants.

The main role of vascular plants as the source of organic matter for PLM samples is confirmed by the AlkTerr value, as found in the Brunei Bay sediments, East Malaysia [20]. The AlkTerr value of PLM 1 samples was 0.39, and PLM 2 was 0.34 (or > 0.3), confirming the main role of vascular plants as the origin of organic matter and indicating the dominance of terrestrial higher plants. The contribution of terrestrial or marine organisms is confirmed by the C_{31}/C_{19} ratio. The value of the C_{31}/C_{19} ratio of each PLM 1 to PLM 5 is 36.81, 15.46, 21.66, 75.35, and 51.35, respectively, which shows that terrestrial organisms are more dominant than marine organisms as a source of organic matter, such as sediments in surface sediments of the Bohai Sea, Yellow Sea, and East China Sea [31].

The C_{29}/C_{17} ratio can also conclude that the source of organic matter comes from the terrestrial or aquatic environment. The C_{29}/C_{17} ratio of PLM 1, PLM 2, and PLM 3 were 32.67, 32.11, and 22.71, respectively, confirming that the source of organic matter is a contribution from the terrestrial environment, such as sediments in surface sediments of the Bohai Sea, Yellow Sea, and East China Sea [29,31]. The C_{17}/C_{31} ratio determined the presence of autochthonous or allochthonous organic matter sources, and the C_{17}/C_{31} ratio of samples PLM 1, PLM 2, and PLM 3 are 0.03, 0.03, and 0.04 respectively, representing allochthonous

sources, such as on the sediments of the East Yellow Sea, Northwest Pacific Ocean, China [22,32].

The ratio of Pr/Ph compounds describes the depositional environment of geological sediments. If the Pr/Ph ratio is more than > 1, it indicates an oxic depositional environment, while a ratio less than < 1 indicates an anoxic depositional environment. A Pr/Ph ratio higher than 1 as an indicator of oxic deposition was reported in the Brunei Bay sediments in Malaysia [20]. Table 2 shows the presence of pristane in PLM 2 and PLM 3, while phytane was only identified in PLM 2 [10,33-34]. The Pr/Ph ratio of the PLM 2 sample yielded a value of 1.26, indicating an oxic depositional environment (Table 3). Based on Pr/n-C_{17} ratio (0.73) and Ph/n-C_{18} ratio (0.36) indicate that PLM 3 is in the oxic region [20]. This ratio has been applied in the Liaodong Bay subbasin, Bohai Bay Basin, China [35].

Triterpenoid

The identification of triterpenoids in the sediment samples based upon the specific fragmentogram m/z 191 confirmed the presence of de-A-lupane compounds and pentacyclic triterpenoids, as observed in Fig. 3 and Table 2.

Table 2 describes the presence of de-A-lupane, $17\beta(H)$-22,29,30-trisnorhopane, $17\beta(H),21\beta(H)$-30-norhopane, and $17\alpha(H),21\beta(H)$-30-homohopane with 22S and 22R configurations in all samples. The $17\alpha(H)$-22,29,30-trisnorhopane (Tm) was only observed in PLM 1 and PLM 5 sediments; olean-12-ene and $17\beta(H),21\beta(H)$-30-homohopane existed in all sample but PLM-4. The $17\alpha(H),21\beta(H)$-30-norhopane was only identified in PLM 4 while the $17\beta(H), 21\beta(H)$-hopane and $17\beta(H),21\alpha(H)$-30-normorethane were only absent in PLM 4. In addition, the gamaserane was only identified in PLM 2.

The presence of triterpenoid compounds was beneficial in determining the source of organic matter from Polaman sediments. De-A-lupane, a non-hopanoid triterpenoid group, was formed due to bacterial activity, resulting in the degradation of the lupane compound during the deposition period. Diagenesis, the compound of lupane, was derived from lupeol as a precursor of vascular plants Angiosperms [36-38]. Therefore, the
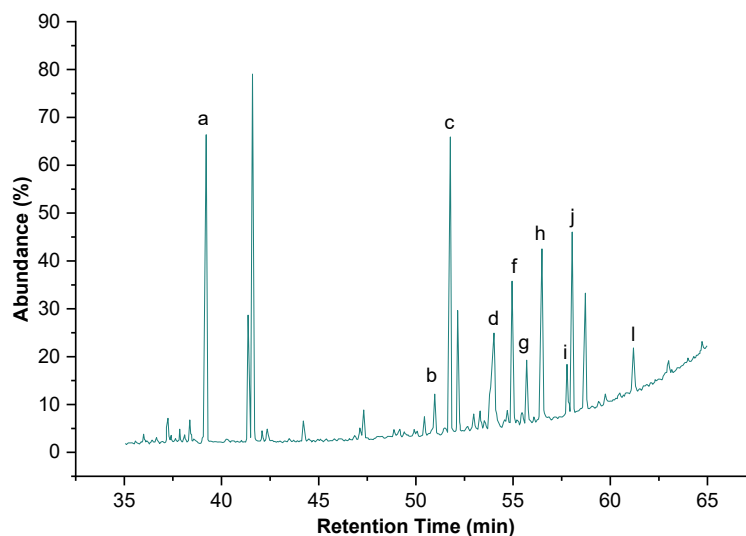
Fig 3. Fragmentogram of pentacyclic sesterterpenoids and triterpenoids on *m/z* 191

presence of de-A-lupane in Polaman sediments affirmed the organic origin from higher terrestrial plants Angiosperms and the presence of bacterial input during sediment deposition [37,39]. This result was also supported by the presence of similar biomarkers in the Bikaner, Nagaur, Jalore, Jaisalmer, and Barmer districts of Rajasthan, western India, and Papua Basin, Papua New Guinea, as indicators of sources of terrestrial higher plant organic matter [40-41]. The origin of organic compounds from Angiosperms was also affirmed by the presence of olean-12-ene compounds in PLM 1, 2, 3, and 5 which derived from β-amirin as a precursor. A similar result was reported in the study of coastal sediments and soils around the city of Tromso [41-42]. The hopanoid triterpenoid compounds in Polaman sediments depicted the presence of C_{27}–C_{30} hopane homologues such as Tm, 17β(*H*)-22,29,30-trisnorhopane, 17α(*H*),21β(*H*)-30-norhopane, 17β(*H*),21β(*H*)-30-norhopane, 17β(*H*),21β(*H*)-hopane, and 17β(*H*),21α(*H*)-30-normorethane. These compounds were derived from the hopanoids diplotene and diplopterol. In addition, there were C_{31} hopane compounds, entitled 17α(*H*),21β(*H*)-30-homohopane with 22*S* and 22*R* configurations, and 17β(*H*),21β(*H*)-30-homohopane originated from bacteriohopanatetrol in the membranes of prokaryotic bacteria [43]. Subsequently, the presence of hopanoid compounds indicated the contribution of bacteria to the source of organic compounds in Polaman sediments. The

contribution from this bacterium was also inferred by the presence of the compound gamacerane, since this compound was associated with dehydrated and hydrogenated tetrahymanol precursors on the protozoan membrane [44-45]. Thus, the identification of gamacerane compounds justified the role of bacteria in the PLM 2 sediment. Hopanoid and gamacerane compounds were also observed in Upper Cretaceous petroleum source rocks from the Gippsland Basin, Australia [8].

The hopanoid compounds in all samples were also employed as an indicator of sample maturity based on the ratio of C_{29} ββ/αβ and C_{31} 22*S*/(22*S* + 22*R*), as written in Table 3. The C_{29} ββ/αβ parameter was calculated based on the ratio of 17α(*H*),21β(*H*)-30-norhopane to 17β(*H*),21β(*H*)-30-norhopane in PLM 4. C_{29} ββ/αβ ratio value > 0.15 confirmed low maturity, while the value < 0.15 inferred high maturity [23,46]. Based on Table 3, PLM 4 exhibited low maturity with the C_{29} ββ/αβ ratio value of 2.24.

Meanwhile, the parameter C_{31} 22*S*/(22*S* + 22*R*) was generated from the ratio of the 22*S* configuration to the sum of the *S* + *R* configurations of 17α(*H*),21β(*H*)-homohopane. The 22*S* configuration of the 17α(*H*),21β(*H*)-homohopane structure is more stable compared to the 22*R* configuration. The low abundance of 17α(*H*),21β(*H*)-homohopane (22*S*) compared to 22*R* indicates a low maturity level. A value of C_{31}22*S*/(22*S* + 22*R*) lower than 1 indicated low maturity, while a value

higher than one affirmed high maturity [5-6,24]. The ratio value of C_{31} 22S/(22 S+ 22R) values for PLM 1 to PLM 5 sediments were 0.22, 0.33, 0.31, 0.35, and 0.30, respectively. All these values demonstrated low maturity. Similar results were also found for Wondama coal, Indonesia, with a ratio value of 0.27 as an indicator of low maturity [6]. The low thermal maturity of the Polaman sediments was also rationalized by the presence of bacterial activity during the sedimentary deposition process. This bacterial activity had been continuing in the early stages of diagenesis, so the presence of bacterial input in the formation of sediment organic matter indicates low maturity of sediment [3,47]. Hopanoid biomarkers are also adopted as indicators of Polaman sediment maturity. The low maturity of sediment was assigned by the presence of 17β(*H*)-22,29,30-trisnorhopane compounds with relatively low structural stability [8,48]. Notably, PLM 4 exhibited high maturity by the presence of 17α(*H*),21β(*H*)-30-norhopane with stable structural over 17β(*H*),21β(*H*)-30-trisnorhopane.

Apart from the indicator of thermal maturity, triterpenoid compounds were capable of determining the depositional environment of Polaman sediments. The formation of De-A-triterpenoids through the degradation of pentacyclic triterpenoids also affirmed the presence of an oxic depositional environment [33-34]. This environment was also pointed by De-A-triterpenoid compounds with the lupane, ursane, and oleanane

structure as the result of photochemical or microbial degradation of pentacyclic triterpenoids. The process was characterized by the release of ring A in the oxidative environment [37]. Therefore, the finding of this compound in Polaman sediments indicates an oxic depositional environment. Gamaserane compounds as indicators of reductive and hypersaline depositional environments were also identified in very low abundance in PLM 2 samples.

Aromatic Hydrocarbon Fraction

The results of the identification of aromatic hydrocarbon fraction biomarkers using GC-MS spectrometer were presented as total ion chromatogram (TIC) in Fig. 4 and their abundance in Table 4. Fig. 3 and Table 4 exhibited alkyl benzene groups, naphthalene derivatives, phenanthrene derivatives, and pentacyclic aromatic triterpenoids as biomarkers. However, alkyl benzene was only observed in PLM 1 and PLM 4 samples.

Alkyl benzene and naphthalene derivatives

Identification of the *m/z* 91 fragmentogram in PLM 4 inferred the presence of eight alkyl benzene compounds such as (4,5-dimethyl)nonylbenzene, (2,7-dimethyl) nonylbenzene, (4,6-dimethyl)decylbenzene, (3,6-dimethyl)decylbenzene, (2,8-dimethyl)decylbenzene, (5,6-dimethyl)undecylbenzene, (2,3,6-trimethyl)decyl benzene, and (3,8-dimethyl)undecylbenzene. The *m/z* 105
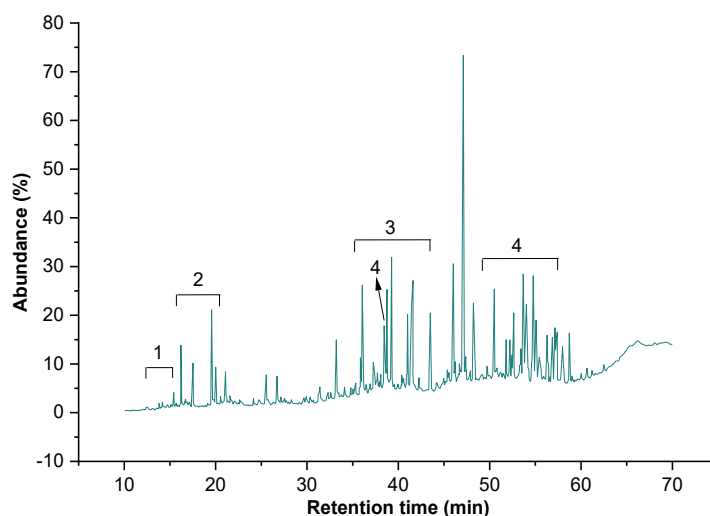
Fig 4. TIC of aromatic hydrocarbon fraction of PLM sediment sample PLM 1-PLM 5. (1) Alkylbenzene, (2) naphthalene derivatives, (3) phenanthrene derivatives, and (4) aromatic pentacyclic triterpenoids

Table 4. The abundance of aromatic hydrocarbon fraction in PLM sediment samples 1-5

Compound name	Molecular formula	Base peak	M⁺	Composition (%)				
				PLM 1	PLM 2	PLM 3	PLM 4	PLM 5
Naphthalene derivatives								
cadalene	$C_{15}H_{18}$	183	198	93.31	100.00	96.58	-	100.00
isocadalene	$C_{15}H_{18}$	183	198	6.69	-	3.42	-	-
norcadalene	$C_{14}H_{16}$	169	184	100.00	-	-	-	-
calamene	$C_{14}H_{16}$	159	202	83.19	100.00	84.05	100.00	-
5,6,7,8-tetrahydrocadalene	$C_{15}H_{22}$	187	202	16.81	-	15.95	-	-
Phenanthrene derivatives								
phenanthrene	$C_{14}H_{10}$	178	178	100.00	100.00	100.00	-	100.00
chrysene	$C_{18}H_{12}$	228	228	-	100.00	-	-	-
3,4,7-trimethyl-1,2,3,4-tetrahydrochrycene	$C_{21}H_{22}$	259	274	59.36	-	100.00	-	-
3,3,7-trimethyl-1,2,3,4-tetrahydrochrycene	$C_{21}H_{22}$	218	274	40.64	-	-	-	-
Aromatic pentacyclic triterpenoids								
dinoroleane-1,3,5(10),12-tetraene	$C_{28}H_{40}$	145	376	44.65	31.06	51.70	-	50.07
dinoursa-1,3,5(10),12-tetraene	$C_{28}H_{40}$	145	376	20.17	-	15.81	-	12.24
dinoroleane-1,3,5(10)-triene	$C_{28}H_{40}$	145	378	35.18	41.30	32.49	-	37.69
dinorlupa-1,3,5(10)-triene	$C_{28}H_{40}$	145	378	-	27.64	-	-	
1,2,4a,9-tetramethyl-1,2,3,4,4a,5,6,14b-octahydropicene	$C_{26}H_{30}$	342	342	75.53	-	64.77	-	82.15
2,2,4a,9-tetramethyl-1,2,3,4,4a,5,6,14b-octahydropicene	$C_{26}H_{30}$	257	342	24.47	-	35.23	-	17.85
8,14-triaromatic secolupane	$C_{27}H_{32}$	169	356	65.64	-	63.88	-	65.28
8,14-triaromatic secooleanane	$C_{27}H_{32}$	169	356	34.36	-	36.12	-	34.72
1,2-dimethyl-1,2,3,4-tetrahydropicene	$C_{24}H_{22}$	295	310	100.00	-	-	-	-
1,2,9-trimethyl-1,2,3,4-tetrahydropicene	$C_{25}H_{24}$	324	324	-	-	42.25	-	-
2,2,9-trimethyl-1,2,3,4-tetrahydropicene	$C_{25}H_{24}$	324	324	-	-	57.75	-	-
Alkyl benzene								
(4,5-dimethyl)nonylbenzene	$C_{17}H_{28}$	91	232	-	-	-	9.20	-
(2,7-dimethyl)nonylbenzene	$C_{17}H_{28}$	91	232	-	-	-	6.44	-
(4,6-dimethyl)decylbenzene	$C_{18}H_{30}$	91	246	-	-	-	19.05	-
(3,6-dimethyl)decylbenzene	$C_{18}H_{30}$	91	246	-	-	-	10.86	-
(2,8-dimethyl)decylbenzene	$C_{18}H_{30}$	91	246	-	-	-	9.19	-
(5,6-dimethyl)undecylbenzene	$C_{19}H_{32}$	91	260	-	-	-	19.89	-
(2,3,6-dimethyl)decylbenzene	$C_{19}H_{32}$	91	260	-	-	-	15.53	-
(3,8-dimethyl)undecylbenzene	$C_{19}H_{32}$	91	260	-	-	-	9.83	-
methyloctylbenzene	$C_{15}H_{24}$	105	204	44.09	-	-	-	-
heptyldimethylbenzene	$C_{15}H_{24}$	119	204	55.91	-	-	-	-
methyldecylbenzene	$C_{17}H_{28}$	105	232	-	-	-	39.32	-
methylundecylbenzene	$C_{18}H_{30}$	105	246	-	-	-	16.21	-
methyldodecylbenzene	$C_{19}H_{32}$	105	260	-	-	-	44.46	-

fragmentogram confirmed the methyl octyl benzene in PLM 1 and PLM 4 possessed methyldecylbenzene, methylundecylbenzene, and methyldodecylbenzene. The *m/z* 119 fragmentogram showed the heptyl dimethylbenzene compounds, an indicator of organic matter derived from carotenoids as precursors produced

by higher terrestrial plants, algae, and cyanobacteria during the diagenesis process. In addition, alkylbenzene compounds also indicated the presence of bacterial activity in the formation of sediment [49-52].

Naphthalene derivatives such as cadalene and isocadelene were identified based on the fragmentogram *m/z* 183, calamene at *m/z* 159, norcadalene at *m/z* 169, and 5,6,7,8,9-tetrahydrocadalene at *m/z* 187. Cadalene compounds were observed in all PLM samples. Isocadalene and 5,6,7,8-tetrahydrocadalene compounds were only identified in PLM 1, PLM 2, and PLM 3. Norcadalene compounds were only found in PLM 1 and 2 while calamene in PLM 1-4. The presence of naphthalene derivatives conveyed the source of organic matter. The abundance of cadalene, isocadalene, and norcadalene compounds in Polaman sediments confirmed the contribution of vascular plants Angiosperms from the Dipterocarpaceae family [4]. Presumably, cadalene was produced by polymerization of polycadinene resins in Dipterocarpaceae plants during the catagenesis stage [53-56]. In addition, the presence of cadalene and isocadalene also justifies the thermal maturity [4]. Isocadalene formed at high temperatures was a more stable isomer than cadalene [57]. Therefore, the high intensity of cadalene compared to isocadalene indicates the low maturity of the Polaman sample [58-59]. A high abundance of the compound cadalene was also found in the coal of the Kutai Basin, Indonesia [53].

The presence of calamene biomarkers and 5,6,7,8-tetrahydrocadalene as derivatives of sesquiterpenoids supported the contribution from Angiosperms plants (Dipterocarpaceae family) and Gymnosperms plants (Cupressaceae family) [57,60-61]. These compounds were also present in rocks Upper Cretaceous petroleum resource, Gipssland Basin, Australia [12].

Phenanthrene derivatives

The phenanthrene group was identified based on the *m/z* 178, 228, 259, and 218 fragmentograms. The presence of phenanthrene compounds in the sediments of PLM 1, PLM 2, PLM 3, and PLM 5 was identified based on the *m/z* 178, conveying Angiosperms and Gymnosperms as the source of organic matter. This compound existed in geological samples of the Middle Miocene [53,62]. The

m/z 228 confirmed the chrysene in PLM 2, the *m/z* 259 assigned 3,4,7-trimethyl-1,2,3,4-tetrahydrochrysene compounds in PLM 1 as well as PLM 3, and the *m/z* 218 for the compound 3,3,7-trimethyl-1,2,3,4-tetrahydrochrysene. These compounds are isomers yet originated from different structural origins. The compound 3,4,7-trimethyl-1,2,3,4-tetrahydrochrysene is derived from ursane, while 3,3,7-trimethyl-1,2,3,4-tetrahydrochrysene is derived from oleanane [39,63-64]. The presence of these compounds confirmed the contribution of Angiosperm plants, which originated from the degradation of β-amyrin in the early stages of diagenesis [61,63,65]. Hence, these two compounds were promising indicators of Angiosperm contribution in Polaman sediment. The existence of these compounds was also found in the Upper Cretaceous petroleum source rocks of the Latrobe Group, Gippsland Basin, Australia [12].

Pentacyclic aromatic triterpenoids

The pentacyclic triterpenoid aromatic compounds in Polaman sediments were identified based on the fragmentograms *m/z* 145, 257, 295, 324, and 356 [10,12,38,40]. The dinoroleane-1,3,5(10),12-tetraene, and dinoroleane-1,3,5(10)-triene in PLM 1, PLM 2, PLM 3, and PLM 5 were studied according to the specific fragmentogram *m/z* 145. Dinorursa-1,3,5(10),12-tetraene biomarkers were identified in PLM 1, PLM 3, and PLM 5, while dinorlupa-1,3,5(10)-triene was only identified in PLM 2 sediments. Dinoroleane-1,3,5(10),12-tetraene, dinorursa-1,3,5(10),12-tetraene, dinoroleane-1,3,5(10)-triene, and dinorlupa-1,3,5(10)-triene are a group of pentacyclic triterpenoid monoaromatic compounds with oleanane, ursane and lupane frame. These compounds were derived from β-amirin and α-amirin as precursors of higher terrestrial plants, especially Angiosperms. It is worth noted only a small number of Gymnosperm plants can produce these compounds [10,66]. Therefore, the presence of these three compounds in Polaman sediments indicates the dominance of organic matter from higher vascular plants, especially Angiosperms. These three compounds were also identified in siliclastic deposits of the Orava-Nowy Targ Basin [66].

Based on the m/z 257 fragmentogram, the 1,2,4a,9-tetramethyl-1,2,3,4,4a,5,6,14b-octahydropysene and 2,2,4a,9-tetramethyl-1,2,3,4,4a,5,6,14b-octahydropycene were observed in PLM 1, PLM 2, and PLM 3. These two compounds indicated that organic matter originated from β-amyrin and α-amyrin as precursors in higher plants Angiosperms [10,40]. The presence of these compounds 1,2,9-trimethyl-1,2,3,4-tetrahydropicene and 2,2,9-trimethyl-1,2,3,4-tetrahydropycene in the analyzed Polaman samples proved of the vascular plant as the source of organic matter [10,53,60]. This pentacyclic tetraaromatic compound was also found in the Eagle Ford Group drilling Central Texas [48]. In addition, PLM 1, PLM 2, PLM 3 consist of 8,14-triaromaticsecolupane and 8,14-triaromaticsecooleanane compounds based on the *m/z* 356 fragmentogram, providing evidence of higher plants Angiosperms as the origin of organic compounds [10,47]. These two compounds were also found in sediments from Mulga Rock, Australia [38]. These two biomarkers were synthesized from the alteration and aromatization of triterpenoids present in Angiosperms during the diagenesis stage. This aromatization process took place as the temperature increased, forming simpler compounds [10,38]. Therefore, the presence of these two biomarkers in the sediment indicated immature samples [10,38,47].

Based on the *m/z* 324 fragmentogram, the biomarkers of 1,2,9-trimethyl-1,2,3,4-tetrahydropycene and 2,2,9-trimethyl-1,2,3,4-tetrahydropycene were identified in PLM 3. Biomarkers formed due to bacterial contribution in the early stages of diagenesis were diagenetic products of β-amyrin, namely pentacyclic triterpenoid with oleanane framework [10,48,53,60]. The same compound was also found in Sangata coal, East Borneo, Kutai Basin coal, and Eagle Ford Group source rock, Texas [10,48,53].

CONCLUSION

Organic geochemical analysis of Polaman sediment samples, the Ngrayong formation as source rock was carried out to determine its potential as an oil and gas producer. Geochemical characteristics are related to the source of organic material, sediment maturity, and ancient depositional environment. The *n*-alkane biomarker with a bimodal distribution in all samples indicated that the organic material came from various sources. Several parameters such as CPI > 1.00, C_{31}/C_{19} ratio > 0.40, Paq 0.37–0.47, and the presence of naphthalene, phenanthrene, and pentacyclic monoaromatic triterpenoid derivatives indicate that the source of organic matter comes from higher plants, algae, and bacteria. This dominant source of terrigenous organic matter is also proven by a TAR value > 1, a C_{29}/C_{17} ratio > 1, and the presence of aromatic hydrocarbon compounds derived from naphthalene, phenanthrene, pentacyclic triterpenoids, and alkyl benzene. Apart from that, the inclusion of bacteria in the formation of organic matter is also proven by the presence of hopanoid compounds. This varied source of organic material is also proven by the C_{17}/C_{31} ratio < 1 as an indicator of allochthonous organic material. The presence of pentacyclic monoaromatic triterpenoids and hopanoids with β isomers indicates low thermal maturity. The oxic deposition environment in the coal formation process is indicated by a Pr/Ph ratio > 1, a high abundance of de-A-lupan. The existence of several biomarkers with the above parameters indicates that coal is a source rock that has the potential to produce oil and gas.

AUTHOR CONTRIBUTIONS

Yulfi Zetra conceptualized research, wrote, and reviewed draft articles. Rafwan Year Perry Burhan conceptualized this work, designed the research methodology, supervised the research, and reviewed the manuscript. Sulistiyono validated the data and reviewed the manuscript. Arizal Firmansyah edited and evaluated

the manuscript. Darin Salsabila collected data, carried out the research methodologies, and wrote the manuscript.

■ **REFERENCES**

[1] Husein, S., Titisari, A.D., Freski, Y.R., and Utama, P.P., 2016, *Buku Panduan Ekskursi Geologi Regional, Jawa Timur Bagian Barat, Indonesia*, Department of Geological Engineering, Faculty of Engineering, UGM, Yogyakarta.

[2] Dhamayanti, E., Raharjanti, N.A., and Hartati, I.A., 2016, Dinamika Sedimentasi Singkapan Formasi Ngrayong dengan Analogi Lingkungan Pengendapan Modern, Studi Kasus Singkapan Polaman dan Braholo dengan Analogi Pesisir Pantai Utara Jawa, *The 9th Seminar Nasional Kebumian*, Grha Sabha Pramana, Yogyakarta, Indonesia, 6-7 October 2016, 725–735.

[3] Killops, S., and Killops, V., 2005, *Introduction to Organic Geochemistry*, 2nd Ed., Blackwell Publishers, Oxford, UK.

[4] Ajuaba, S., Sachsenhofer, R.F., Meier, V., Gross, D., Schnyder, J., Omodeo-Salé, S., Moscariello, A., and Misch, D., 2023, Coaly and lacustrine hydrocarbon source rocks in Permo-Carboniferous graben deposits (Weiach well, Northern Switzerland), *Mar. Petrol. Geol.*, 150, 106147.

[5] Cieślik, E., and Fabiańska, M.J., 2021, Preservation of geochemical markers during co-combustion of hard coal and various domestic waste materials, *Sci. Total Environ.*, 768, 144638.

[6] Zetra, Y., Burhan, R.Y.P., Pratama, A.D., and Wahyudi, A., 2020, Origin and maturity of biomarker aliphatic hydrocarbon in Wondama coal Indonesia, *J. Idn. Chem. Soc.*, 3 (2), 107–116.

[7] Kumar, S., Dutta, S., and Bhui, U.K., 2021, Provenance of organic matter in an intracratonic rift basin: Insights from biomarker distribution in Palaeogene crude oils of Cambay Basin, western India, *Org. Geochem.*, 162, 104329.

[8] Jiang, L. and George, S.C., 2018, Biomarker signatures of Upper Cretaceous Latrobe Group hydrocarbon source rocks, Gippsland Basin, Australia: Distribution and palaeoenvironment

significance of aliphatic hydrocarbons, *Int. J. Coal Geol.*, 196, 29–42.

[9] Zhu, Z., Li, M., Li, J., Qi, L., Liu, X., Xiao, H., and Leng, J., 2022, Identification, distribution and geochemical significance of dinaphthofurans in coals. *Org. Geochem*, *166*, 104399.

[10] Nádudvari, Á., Misz-Kennan, M., Fabiańska, M., Ciesielczuk, J., Krzykawski, T., Simoneit, B.R.T., and Marynowski, L., 2023, Preservation of labile organic compounds in sapropelic coals from the Upper Silesian Coal Basin, Poland, *Int. J. Coal Geol.*, 267, 104186.

[11] Fang, R., Littke, R., Zieger, L., Baniasad, A., Li, M., and Schwarzbauer, J., 2019, Changes of composition and content of tricyclic terpane, hopane, sterane, and aromatic biomarkers throughout the oil window: A detailed study on maturity parameters of Lower Toarcian Posidonia Shale of the Hils Syncline, NW Germany, *Org. Geochem.*, 138, 103928.

[12] Jiang, L., and George, S.C., 2019, Biomarker signatures of Upper Cretaceous Latrobe Group petroleum source rocks, Gippsland Basin, Australia: Distribution and geological significance of aromatic hydrocarbons, *Org. Geochem.*, 138, 103905.

[13] Simoneit, B.R.T., Oros, D.R., Karwowski, Ł., Szendera, Ł., Smolarek-Lach, J., Goryl, M., Bucha, M., Rybicki, M., and Marynowski, L., 2020, Terpenoid biomarkers of ambers from Miocene tropical paleoenvironments in Borneo and of their potential extant plant sources, *Int. J. Coal Geol.*, 221, 103430.

[14] Nádudvari, Á., Forzese, M., Maniscalco, R., Di Stefano, A., Misz-Kennan, M., Marynowski, L., Krzykawski, T., and Simoneit, B.R.T., 2022, The transition toward the Messinian evaporites identified by biomarker records in the organic-rich shales of the Tripoli Formation (Sicily, Italy), *Int. J. Coal Geol.*, 260, 104053.

[15] Körmös, S., Sachsenhofer, R.F., Bechtel, A., Radovics, B.G., Milota, K., and Schubert, F., 2021, Source rock potential, crude oil characteristics and oil-to-source rock correlation in a Central Paratethys sub-basin, the Hungarian Palaeogene

Basin (Pannonian basin), *Mar. Pet. Geol.*, 127, 104955.

[16] El-Sabagh, S.M., El-Naggar, A.Y., El Nady, M.M., Ebiad, M.A., Rashad, A.M., and Abdullah, E.S., 2018, Distribution of triterpanes and steranes biomarkers as indication of organic matters input and depositional environments of crude oils of oilfields in Gulf of Suez, Egypt, *Egypt. J. Pet.*, 27 (4), 969–977.

[17] Lee, D.H., Kim, S.H., Choi, J., Kang, N.K., Hwang, I.G., and Shin, K.H., 2022, Geochemical signatures of organic matter associated with gas generation in the Pohang Basin, South Korea, *Geosci. J.*, 26 (5), 555–567.

[18] Chen, Q., Guo, Z., Yu, M., Sachs, J.P., Hou, P., Li, L., Jin, G., Liu, Y., and Zhao, M., 2021, Lipid biomarker estimates of seasonal variations of aerosol organic carbon sources in coastal Qingdao, China, *Org. Geochem.*, 151, 104148.

[19] Zetra, Y., Burhan, R.Y.P., Firdaus, A.W., Nugrahaeni, Z.V., and Gunawan, T., 2021, Characteristics of Cepu block oil, Wonocolo formation, East Java Indonesia: Study of aliphatic biomarkers, *AIP Conf. Proc.,* 2349 (1), 020040.

[20] Pang, S.Y., Suratmman, S., Tay, J.H., and Mohd Tahir, N., 2021, Investigation of aliphatic and polycyclic aromatic hydrocarbons in surface sediments of Brunei Bay, East Malaysia, *Asian J. Chem.*, 33 (2), 439–446.

[21] de Sousa, A.A.C., Sousa, E.S., Rocha, M.S., Sousa Junior, G.R., de Souza, I.V.A.F., Brito, A.S., Souza, S.S., Lopes, J.A.D., Nogueira, A.C.R., and de Lima, S.G., 2020, Aliphatic and aromatic biomarkers of the Devonian source rocks from the Western Parnaíba Basin Brazil: Pimenteiras formation, *J. South Am. Earth Sci.*, 99, 102493.

[22] Jin, J., Guo, H., Gao, Z., Mao, R., and Lu, H., 2022, Biodegradation of dissolved organic matter and sedimentary organic matter in high arsenic groundwater system: Evidence from lipid biomarkers and compound-specific carbon isotopes, *Chem. Geol.*, 612, 121140.

[23] Kang, S., Shao, L., Qin, L., Li, S., Liu, J., Shen, W., Chen, X., Eriksson, K.A., and Zhou, Q., 2020, Hydrocarbon generation potential and depositional

setting of Eocene oil-prone coaly source rocks in the Xihu Sag, East China Sea Shelf Basin, *ACS Omega*, 5 (50), 32267–32285.

[24] Patra, S., Dirghangi, S.S., Rudra, A., Dutta, S., Ghosh, S., Varma, A.K., Shome, D., and Kalpana, M.S., 2018, Effects of thermal maturity on biomarker distributions in Gondwana coals from the Satpura and Damodar Valley Basins, India, *Int. J. Coal Geol.*, 196, 63–81.

[25] Herrera-Herrera, A.V., Leierer, L., Jambrina-Enríquez, M., Connolly, R., and Mallol, C., 2020, Evaluating different methods for calculating the Carbon Preference Index (CPI): Implications for palaeoecological and archaeological research, *Org. Geochem.*, 146, 104056.

[26] Yu, X., Lü, X., Meyers, P.A., and Huang, X., 2021, Comparison of molecular distributions and carbon and hydrogen isotope compositions of *n*-alkanes from aquatic plants in shallow freshwater lakes along the middle and lower reaches of the Yangtze River, China, *Org. Geochem.*, 158, 104270.

[27] Bliedtner, M., Schäfer, M.I.K., Zech, R., and von Suchodoletz, H., 2018, Leaf wax *n*-alkanes in modern plants and topsoils from eastern Georgia (Caucasus) – Implications for reconstructing regional paleovegetation, *Biogeosciences,* 15 (12), 3927–3936.

[28] Ceccopieri, M., Scofield, A.L., Almeida, L., and Wagener, A.L.R., 2018, Compound-specific δ^{13}C of *n*-alkanes: Clean-up methods appraisal and application to recent sediments of a highly contaminated bay, *J. Braz. Chem. Soc.*, 29 (11), 2363–2377.

[29] Ratheesh Kumar, C.S., Renjith, K.R., Joseph, M.M., Salas, P.M., Resmi, P., and Chandramohanakumar, N., 2019, Inventory of aliphatic hydrocarbons in a tropical mangrove estuary: A biomarker approach, *Environ. Forensics*, 20 (4), 370–384.

[30] Imfeld, A., Ouellet, A., Douglas, P.M.J., Kos, G., and Gélinas, Y., 2022, Molecular and stable isotope analysis (δ^{13}C, δ^{2}H) of sedimentary *n*-alkanes in the St. Lawrence Estuary and Gulf, Quebec, Canada: Importance of even numbered *n*-alkanes in coastal

systems, *Org. Geochem.*, 164, 104367.

[31] Zou, Y., Wang, C., Liu, X., and Wang, H., 2022, Spatial distribution, compositional pattern and source apportionment of *n*-alkanes in surface sediments of the Bohai Sea, Yellow Sea, and East China Sea and implications of carbon sink, *Mar. Pollut. Bull.*, 178, 113639.

[32] Özdemir, A., Palabiyik, Y., Karataş, A., and Şahinoğlu, A., 2022, Mature petroleum hydrocarbons contamination in surface and subsurface waters of Kızılırmak Graben (Central Anatolia, Turkey): Geochemical evidence for a working petroleum system associated with a possible salt diapir, *Turk. J. Eng.*, 6 (1), 1–15.

[33] Zhu, Z., Li, M., Li, J., Qi, L., Liu, X., Xiao, H., and Leng, J., 2022, Identification, distribution and geochemical significance of dinaphthofurans in coals, *Org. Geochem.*, 166, 104399.

[34] Al-Areeq, N.M., Al-Badani, M.A., Salman, A.H., and Albaroot, M.A., 2018, Petroleum source rocks characterization and hydrocarbon generation of the Upper Jurassic succession in Jabal Ayban field, Sabatayn Basin, Yemen, *Egypt. J. Pet.*, 27 (4), 835, 835–851.

[35] Wang, N., Xu, Y., Li, W., Wang, F., Chen, G., Liu, Y., Cheng, R., and Liu, H., 2022, The compositions of biomarkers and macerals in the first member of the Shahejie Formation in the Liaodong Bay subbasin, Bohai Bay Basin: Implications for biological sources and seawater incursions, *J. Pet. Sci. Eng.*, 218, 110947.

[36] Schaeffer, P., Bailly, L., Motsch, E., and Adam, P., 2019, The effects of diagenetic aromatization on the carbon and hydrogen isotopic composition of higher plant di- and triterpenoids: Evidence from buried wood, *Org. Geochem.*, 136, 103889.

[37] Lopes, A.A., Pereira, V.B., Amora-Nogueira, L., Marotta, H., Moreira, L.S., Cordeiro, R.C., Vanini, G., and Azevedo, D.A., 2021, Hydrocarbon sedimentary organic matter composition from different water-type floodplain lakes in the Brazilian Amazon, *Org. Geochem.*, 159. 104287.

[38] Greenwood, P.F., Shan, C., Holman, A.I., and Grice, K., 2018, The composition and radiolysis impact on aromatic hydrocarbons in sedimentary organic matter from the Mulga Rock (Australia) uranium deposit, *Org. Geochem.*, 123, 103–112.

[39] Wang, N., Xu, Y.H., Wang, F.L., Liu, Y., Huang, Q., and Huang, X., 2022, Identification and geochemical significance of unusual C_{24} tetracyclic terpanes in Shahejie Formation source rocks in the Bozhong subbasin, Bohai Bay Basin, *Pet. Sci.*, 19 (5), 1993–2003.

[40] Xu, M., Hou, D., Lin, X., Liu, J., Ding, W., and Xie, R., 2022, Organic geochemical signatures of source rocks and oil-source correlation in the Papuan Basin, Papua New Guinea, *J. Pet. Sci. Eng.*, 210, 109972.

[41] Kumar, D., Ghosh, S., Tiwari, B., Varma, A.K., Mathews, R.P., and Chetia, R., 2021, Palaeocene-Eocene organic sedimentary archives of Bikaner-Nagaur Basin, Rajasthan, India: An integrated revelation from biogeochemical and elemental proxies, *Int. J. Coal Geol.*, 247, 103848.

[42] Morgunova, I., Kursheva, A., Petrova, V., Litvinenko, I., Batova, G., and Renaud, P., 2019, Hydrocarbon Monitoring in Coastal Sediments and Soils Around the City of Tromsø: Complex Molecular Geochemical Approach, *The 29th International Meeting on Organic Geochemistry (IMOG)*, European Association of Organic Geochemist, Gothenburg, Sweden, 1-6 September 2019, 1–2.

[43] Synnott, D.P., Schwark, L., Dewing, K., Percy, E.L., and Pedersen, P.K., 2021, The diagenetic continuum of hopanoid hydrocarbon transformation from early diagenesis into the oil window, *Geochim. Cosmochim. Acta*, 308, 136–156.

[44] Liu, B., Vrabec, M., Markič, M., and Püttmann, W., 2019, Reconstruction of paleobotanical and paleoenvironmental changes in the Pliocene Velenje Basin, Slovenia, by molecular and stable isotope analysis of lignites, *Int. J. Coal Geol.*, 206, 31–45.

[45] Cordova-Gonzalez, A., Birgel, D., Kappler, A., and Peckmann, J., 2020, Carbon stable isotope patterns of cyclic terpenoids: A comparison of cultured alkaliphilic aerobic methanotrophic bacteria and methane-seep environments, *Org. Geochem.*, 139, 103940.

[46] Samad, S.K., Mishra, D.K., Mathews, R.P., Ghosh, S., Mendhe, V.A., and Varma, A.K., 2020, Geochemical attributes for source rock and palaeoclimatic reconstruction of the Auranga Basin, India, *J. Pet. Sci. Eng.*, 185, 106665.

[47] Nakamura, H., 2019, Plant-derived triterpenoid biomarkers and their applications in paleoenvironmental reconstructions: Chemotaxonomy, geological alteration, and vegetation reconstruction, *Org. Geochem.*, 35 (2), 11–35.

[48] French, K.L., Birdwell, J.E., and Whidden, K.J., 2019, Geochemistry of a thermally immature Eagle Ford Group drill core in central Texas, *Org. Geochem.*, 131, 19–33.

[49] Plet, C., Grice, K., Scarlett, A.G., Ruebsam, W., Holman, A.I., and Schwark, L., 2020, Aromatic hydrocarbons provide new insight into carbonate concretion formation and the impact of eogenesis on organic matter, *Org. Geochem.*, 143, 103961.

[50] French, K.L., Birdwell, J.E., and Vanden Berg, M.D., 2020, Biomarker similarities between the saline lacustrine Eocene Green River and the Paleoproterozoic Barney Creek Formations, *Geochim. Cosmochim. Acta*, 274, 228–245.

[51] Xiao, H., Li, M., Wang, T., You, B., Lu, X., and Wang, X., 2022, Organic molecular evidence in the ~1.40 Ga Xiamaling Formation black shales in North China Craton for biological diversity and paleoenvironment of mid-Proterozoic ocean, *Precambrian Res.*, 381, 106848.

[52] Ghosh, S., Dutta, S., Bhattacharyya, S., Konar, R., and Priya, T., 2022, Paradigms of biomarker and PAH distributions in lower Gondwana bituminous coal lithotypes, *Int. J. Coal Geol.*, 260, 104067.

[53] Jiang, L., Ding, W., and George, S.C., 2020, Late Cretaceous–Paleogene palaeoclimate reconstruction of the Gippsland Basin, SE Australia, *Palaeogeogr., Palaeoclimatol., Palaeoecol.*, 556, 109885.

[54] Kumar, S., and Dutta, S., 2021, Utility of comprehensive GC×GC-TOFMS in elucidation of aromatic hydrocarbon biomarkers, *Fuel*, 283, 118890.

[55] Burhan, R.Y.P., Zetra, Y., and Amini, Y.A., 2020, Paleoenvironmental and maturity indicator of Cepu Block Oil, Wonocolo Formation, East Java Indonesia, *Jurnal Teknologi*, 82 (5), 173–182.

[56] Murillo, W.A., Horsfield, B., and Vieth-Hillebrand, A., 2019, Unraveling petroleum mixtures from the South Viking Graben, North Sea: A study based on $\delta^{13}C$ of individual hydrocarbons and molecular data, *Org. Geochem.*, 137, 103900.

[57] Lopes Martins, L., Schulz, H.M., Portugal Severiano Ribeiro, H.J., Adolphsson do Nascimento, C., Soares de Souza, E., and Feitosa da Cruz, G., 2020, Cadalenes and norcadalenes in organic-rich shales of the Permian Irati Formation (Paraná Basin, Brazil): Tracers for terrestrial input or also indicators of temperature-controlled organic-inorganic interactions, *Org. Geochem.*, 140, 103962.

[58] Petersen, H.I., Fyhn, M.B.W., Nytoft, H.P., Dybkjær, K., and Nielsen, L.H., 2022, Miocene coals in the Hanoi trough, onshore northern Vietnam: Depositional environment, vegetation, maturity, and source rock quality, *Int. J. Coal Geol.*, 253, 103953.

[59] Li, Z., Huang, H., and George, S.C., 2022, Organic Geochemistry Unusual occurrence of alkylnaphthalene isomers in upper Eocene to Oligocene sediments from the western margin of Tasmania, Australia, *Org. Geochem.*, 168, 104418.

[60] Ding, W., Hou, D., Gan, J., Zhang, Z., and George, S.C., 2022, Aromatic hydrocarbon signatures of the late Miocene-early Pliocene in the Yinggehai Basin, South China Sea: Implications for climate variations, *Mar. Petrol. Geol.*, 142, 105733.

[61] Simoneit, B.R.T., Otto, A., Menor-Sálvan, C., Oros, D.R., Wilde, V., and Riegel, W., 2021, Composition of resinites from the Eocene Geiseltal brown coal basin, Saxony-Anhalt, Germany and comparison to their possible botanical analogues, *Org. Geochem.*, 152, 104138.

[62] Lu, Z., Li, Q., Ju, Y., Gu, S., Xia, P., Gao, W., Yan, Z., and Gong, C., 2022, Biodegradation of coal organic matter associated with the generation of secondary biogenic gas in the Huaibei Coalfield, *Fuel*, 323,

124281.

[63] Walters, C.C., Wang, F.C., Higgins, M.B., and Madincea, M.E., 2018, Universal biomarker analysis: Aromatic hydrocarbon, *Org. Geochem.*, 124, 205–214.

[64] Wakeham, S.G., and Canuel, E.A., 2016, Biogenic polycyclic aromatic hydrocarbons in sediments of the San Joaquin River in California (USA), and current paradigms on their formation, *Environ. Sci. Pollut. Res.*, 23 (11), 10426–10442.

[65] El Diasty, W.S., Peters, K.E., Moldowan, J.M., Essa, G.I., and Hammad, M.M., 2020, Organic geochemistry of condensates and natural gases in the northwest Nile Delta offshore Egypt, *J. Pet. Sci. Eng.*, 187, 106819.

[66] Jaroszewicz, E., Bojanowski, M., Marynowski, Łoziński, M.L., and Wysocka, A., 2018, Paleoenvironmental conditions, source and maturation of Neogene organic matter from the siliciclastic deposits of the Orava-Nowy Targ Basin, *Int. J. Coal Geol.*, 196, 288–301.